Anthropogenic Weakening of the Tropical Circulation: The Relative Roles of Direct CO_2 Forcing and Sea Surface Temperature Change

JIE HE AND BRIAN J. SODEN

Rosenstiel School of Marine and Atmospheric Science, University of Miami, Miami, Florida

ABSTRACT

There is a lack of consensus on the physical mechanisms that drive the anthropogenic weakening of tropical circulation. This study investigates the relative roles of direct CO_2 forcing, mean SST warming, and the pattern of SST change on the weakening of the tropical circulation using an ensemble of AMIP and aquaplanet simulations. In terms of the mean weakening of the tropical circulation, the SST warming dominates over the direct CO_2 forcing through its control over the tropical mean hydrological cycle and tropospheric stratification. In terms of the spatial pattern of circulation weakening, however, the three forcing agents are all important contributors, especially over the ocean. The increasing CO_2 weakens convection over ocean directly by stabilizing the lower troposphere and indirectly via the land–sea warming contrast. The mean SST warming drives strong weakening over the centers and edges of convective zones. The pattern of SST warming plays a crucial role on the spatial pattern of circulation weakening over the tropical Pacific.

The anthropogenic weakening of the Walker circulation is mostly driven by the mean SST warming. Increasing CO_2 strengthens the Walker circulation through its indirect effect on land–sea warming contrast. Changes in the upper-level velocity potential indicate that the pattern of SST warming does not weaken the Walker circulation despite being "El Niño–like." A weakening caused by the mean SST warming also dominates changes in the Hadley circulation in the AMIP simulations. However, this weakening is not simulated in the Southern Hemisphere in coupled simulations.

1. Introduction

The atmospheric circulation plays a critical role in climate, influencing the global distributions of precipitation and temperature. A general weakening of tropical circulation has emerged unambiguously in model simulations of anthropogenic climate change (e.g., Held and Soden 2006; Vecchi and Soden 2007; Chadwick et al. 2013a; Kociuba and Power 2015) and has been detected in observations of the past half-century (e.g., Vecchi et al. 2006; Collins et al. 2010; Tokinaga et al. 2012), although the latter is partly due to natural variability (e.g., Power and Smith 2007; Power and Kociuba 2011; Meng et al. 2012).

The anthropogenic weakening of the tropical circulation can be explained from both thermodynamic and dynamic points of view. Thermodynamically, the faster increase in atmospheric moisture than precipitation requires the general weakening of the circulation (Held and Soden 2006). Dynamically, the weakening of tropical circulation can be expected as a result of the balance between convective heating, radiative cooling and increasing stratification (Knutson and Manabe 1995) or the vertical advection of stratification change (Ma et al. 2012). It may also reflect an enhanced gross moist stability (Chou and Neelin 2004) or the "upped ante" mechanism (Neelin et al. 2003; Chou et al. 2009) on a regional scale.

Although these mechanisms have helped understand the anthropogenic weakening of tropical circulation, the direct physical driver of the weakening is still a subject of ongoing investigation. Because the circulation weakens as the climate warms, one may intuitively consider the weakening to be mostly driven by surface warming. However, Bony et al. (2013) found that a substantial portion of the circulation change occurred immediately

---

Corresponding author address: Jie He, Rosenstiel School of Marine and Atmospheric Science, University of Miami, 4600 Rickenbacker Causeway, Miami, FL 33149.
E-mail: jhe@rsmas.miami.edu

in the abrupt quadruple CO_2 simulations when the surface has barely warmed. This indicates that the change in circulation is largely driven by the direct CO_2 forcing. Other studies have also shown a weakening of circulation under direct CO_2 forcing (e.g., Andrews et al. 2009; Chadwick et al. 2013b; Thorpe and Andrews 2014).

However, Chadwick et al. (2014) argued that the fast changes in circulation shown by Bony et al. (2013) were mostly driven by the pattern of sea surface temperature (SST) change, whereas the direct CO_2 forcing only contributed slightly. This indicates that the spatial weakening of circulation might be associated with the pattern of SST change. The importance of the pattern of SST change as a driver of circulation weakening has also been demonstrated in observations (e.g., Tokinaga et al. 2012).

This study aims to determine the relative roles of the direct CO_2 forcing, the mean SST warming, and the pattern of SST change in weakening the tropical circulation. Coupled climate models can be insightful for understanding the circulation change since they include both the direct effect of increasing CO_2 and the indirect effects through changes in SST. However, they are not ideal for the purpose of attribution. In this study, we isolate the effect of different kinds of forcing by means of ensemble AGCM simulations, in which only one forcing agent is specified. This technique allows us to establish a direct causal relationship between the forcing agents and changes in the atmospheric circulation. Although AGCM simulations of natural climate variability have been long criticized for their lack of coupling with an underlying ocean, He and Soden (2015) showed that the lack of ocean coupling has no effect on simulations of anthropogenic climate change (i.e., AGCMs are able to perfectly reproduce the anthropogenic climate change from CGCMs despite the lack of energetically consistent surface fluxes), lending credence to our approach.

The use of AGCM simulations with a single forcing agent has been applied to compare the individual impacts of direct atmospheric radiative forcing and SST change on the climate trend of the past half-century (e.g., Bracco et al. 2004; Compo and Sardeshmukh 2009; Deser and Phillips 2009). Most of these studies found approximately equal importance of direct atmospheric radiative forcing and SST change, although their results were susceptible to internal variability (Deser et al. 2012). Similar techniques have also been applied to investigate certain aspects of anthropogenic changes in tropical circulation. For example, He et al. (2014) showed that the response of vertical velocity at 500 hPa to a uniform SST warming generally opposed its climatology, indicating a weakening effect of the mean

surface warming. Using the uncoupled GFDL model, Ma et al. (2012) showed that the mean SST warming weakened the Walker circulation, whereas the direct CO_2 forcing strengthened it. This strengthening effect of CO_2 is contradictory to the commonly assumed stabilizing effect of CO_2 (e.g., Bony et al. 2013; Thorpe and Andrews 2014) and could be associated with the land–sea warming contrast (e.g., Joshi et al. 2008; Bayr and Dommenget 2013; Chadwick et al. 2014). Our study seeks to extend and reconcile previous studies by offering a thorough investigation of the individual impacts of the direct CO_2 forcing, mean SST warming, and pattern of SST warming on the weakening of tropical circulation.

2. Data and methods

a. Model simulations

We analyze the monthly output of coupled and atmosphere-only simulations from phase 5 of the Coupled Model Intercomparison Project (CMIP5) archive (Taylor et al. 2012). The coupled simulations are forced with the "1pctCO2" scenario and represent the total effect of direct CO_2 forcing and SST changes. We define the mean climate as the average of years 1 to 20 and the perturbed climate as the average of years 121 to 140.

The atmosphere-only simulations are 1) the AMIP control simulations (AMIP_ctrl), which are run from years 1979 to 2008 forced with the observed monthly mean SST and sea ice concentration; 2) the CO_2 only simulations (AMIP_CO2), which are the same as AMIP_ctrl except that the atmospheric CO_2 concentration is quadrupled; 3) the mean SST increase simulations (AMIP_mean), which are the same as AMIP_ctrl except adding a uniform +4-K SST anomaly; and 4) the structured SST increase simulations (AMIP_future), which are the same as AMIP_ctrl except adding the SST anomalies as the composite of the SST responses taken from the coupled model CMIP3 experiments at the time of CO_2 quadrupling. Note that the land warms slightly in the AMIP_CO2 simulation as a result of the direct CO_2 forcing (Fig. 1c); likewise, the land warms slightly less in the AMIP_mean simulation than the 1pctCO2 simulation (Figs. 1a,d) due to the lack of direct CO_2 forcing (Compo and Sardeshmukh 2009). To eliminate the impact from differences in land warming, we also analyze an ensemble of aquaplanet simulations forced with quadruple CO_2 (aqua_CO2) and 4-K uniform warming (aqua_mean). The aquaplanet simulations are run for 5 years with prescribed SST.

To equalize the magnitude of CO_2 and SST forcing in the coupled and AMIP simulations, climate changes in
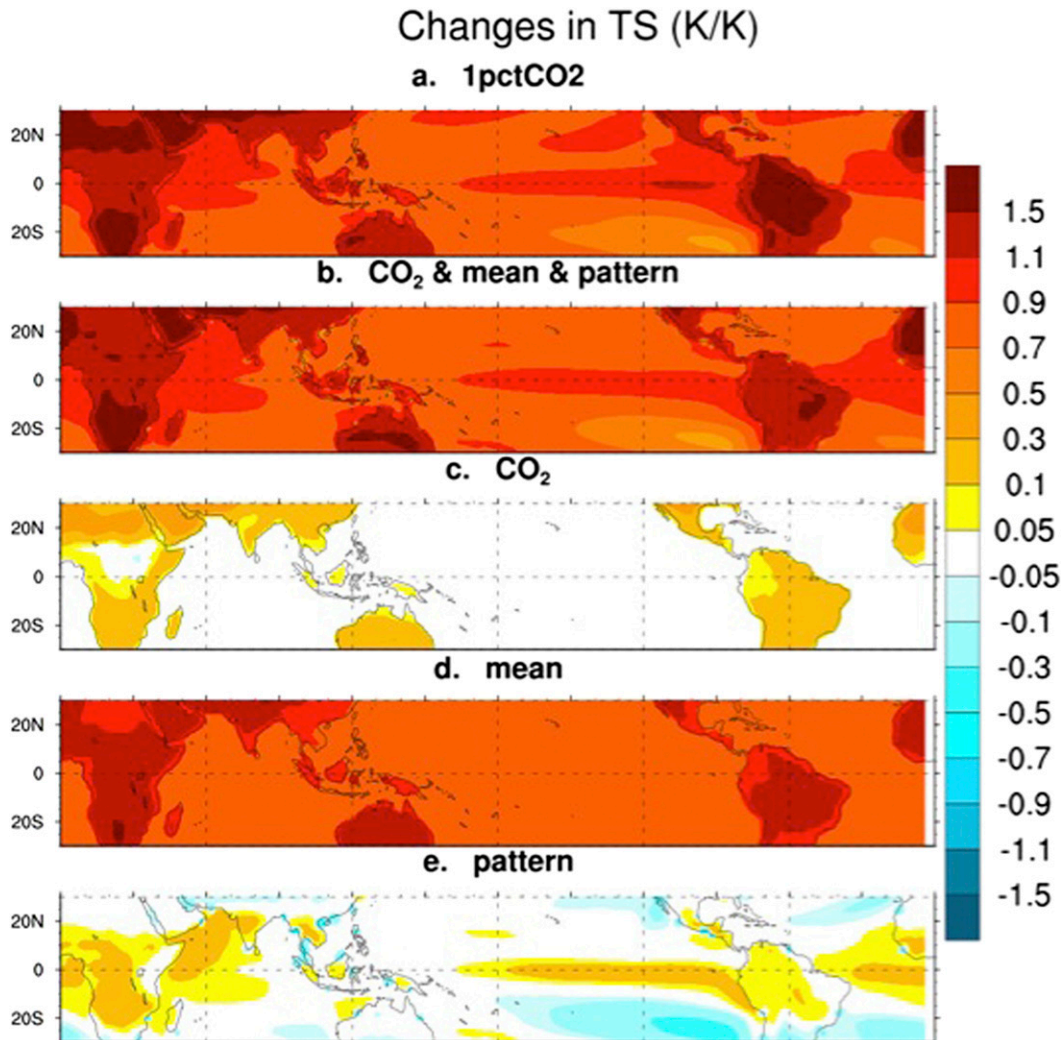
Changes in TS (K/K)

FIG. 1. Ensemble mean changes in the tropical surface temperature from (a) 1pctCO2, (b) sum of AMIP_CO2, AMIP_mean, and AMIP_pattern, (c) AMIP_CO2, (d) AMIP_mean, and (e) AMIP_pattern. Changes are normalized by each model's tropical mean surface temperature changes in the 1pctCO2 simulation before they are averaged across models to yield an ensemble mean. Note that the shading levels are not of equal intervals.

the AMIP simulations are first scaled linearly to match the CO_2 and tropical SST forcing in the 1pctCO2 simulations. Specifically, the changes from the quadrupled AMIP_CO2 simulation are multiplied by a factor of 3.3/4.0 to account for the smaller increase in CO_2 (which increases by only a factor of 3.3 between years 1 and 120) in the 1pctCO2 simulation; that is, we assume that the climate responds linearly to increasing CO_2. Finally, climate change is normalized by each model's tropical mean surface temperature change in the 1pctCO2 simulation and then averaged across models to yield a multimodel ensemble mean, in order to avoid dominance by models with large climate sensitivity.

The effect of the pattern of SST change is estimated by subtracting the climate changes in AMIP_mean from

AMIP_future; we refer to the residual as AMIP_pattern. Although the pattern of SST change in the AMIP_pattern simulation could vary from that in the 1pctCO2 simulation for an individual model, the ensemble mean pattern of tropical SST change is very similar in the two simulations (Figs. 1a and 1b, with a spatial correlation of 0.89). Therefore, we consider the ensemble mean effect of the pattern of SST change to be well represented by the AMIP_pattern simulation.

Nine CGCMs and their AGCM counterparts are used for the coupled and AMIP simulations: BCC-CSM1.1, CanESM2/CanAM4, CNRM-CM5, HadGEM2-ES/HadGEM2-A, IPSL-CM5B-LR, MIROC5, MPI-ESM-LR, MPI-ESM-MR, and MRI-CGCM3. Six models are used for the aquaplanet simulations, namely CCSM4,

CNRM-CM5, IPSL-CM5A-LR, MPI-ESM-LR, MPI-ESM-MR, and MRI-CGCM3. One realization is used from each model. Details about the model simulations can be found online at http://cmip-pcmdi.llnl.gov/cmip5/getting_started_CMIP5_experiment.html. Model data and descriptions can be found at http://pcmdi3.llnl.gov/esgcet/home.htm and expansions of acronyms are available online at http://www.ametsoc.org/PubsAcronymList.

b. Convective mass flux

We analyze the weakening of tropical circulation mainly through changes in the convective mass flux. Unfortunately, model-simulated convective mass flux is not available for all the simulations. However, as convective rainfall dominates over large-scale rainfall in the tropics, we can constrain the convective mass flux through precipitation and boundary layer moisture (Held and Soden 2006):

$$M^* = P/q, \tag{1}$$

where P, q, and M^* are precipitation, near-surface specific humidity, and the equivalent convective mass flux, respectively. Previous studies have shown that M^* is a valid approximation to the model-simulated convective mass flux both in terms of tropical mean (Held and Soden 2006; Vecchi and Soden 2007) and spatial distribution (Chadwick et al. 2013a). Spatial changes in M^* are equivalent to spatial changes in the vertically integrated convective mass flux, with exceptions over steep orography in the Himalayas and Andes (Chadwick et al. 2013a).

3. Results

a. Tropical mean convective mass flux change

We begin our analysis of the tropical circulation weakening by examining changes in the tropical mean convective mass flux. Following Held and Soden (2006), we derive the proportional change in tropical mean convective mass flux as the difference between the proportional change in tropical mean precipitation and the proportional change in tropical mean near-surface moisture:

$$\frac{\partial M^*}{M^*} = \frac{\partial P}{P} - \frac{\partial q}{q}. \tag{2}$$

Figure 2 shows the proportional changes in tropical mean precipitation, moisture, and convective mass flux from the 1pctCO2 simulation and AMIP simulations. In the 1pctCO2 simulation (Fig. 2a), the tropical mean moisture increases at 6.7% K^{-1}, close to the Clausius–Clapeyron relation, whereas the mean precipitation increases at

1.2% K^{-1}, as determined by the rate of atmospheric radiative cooling (e.g., Boer 1993; Soden 2000; Allen and Ingram 2002). The difference between the rate of moistening and rate of precipitation increase requires that the tropical mean convection weakens at 5.5% K^{-1} (Held and Soden 2006).

As shown in Fig. 2, the sum of the hydrological changes in the AMIP_CO2, AMIP_mean, and AMIP_pattern simulations is very close to those in the 1pctCO2 simulation, indicating the linearity of the hydrological changes. However, these changes are very unevenly distributed in the AMIP simulations. The pattern of SST change has virtually no effect on the topical mean hydrological cycle (Fig. 2d). The slight increase in moisture is likely associated with the equator–subtropical gradient in SST warming, which favors moistening in the lower latitudes (Xie et al. 2010). As a result, the tropical mean convection weakens slightly but only accounts for less than 4% of the total weakening.

In the AMIP_CO2 simulation (Fig. 2b), the near surface moisture increases at 0.5% K^{-1} as a result of the increase of the atmospheric temperature, whereas precipitation decreases at 1.2% K^{-1} due to the atmospheric radiative warming. This causes the mean convection to weaken at -1.6% K^{-1}, which accounts for about 30% of the total weakening. Because the land surface temperature is not fixed and warms slightly in the AMIP_CO2 simulation (Fig. 1c), the weakening of convection could be attributed to both the direct CO_2 forcing and land–sea warming contrast, which shifts convection from ocean to land (Chadwick et al. 2014; discussed later in section 3). To eliminate the effect of land warming, we also analyze the direct CO_2 influence in the aqua_CO2 simulation. As shown in Fig. 2b, both the moistening and precipitation decrease is moderately reduced when the effect of land warming is removed, but the mean convection still weakens albeit at a smaller rate.

The mean SST warming is the dominant driver of changes in the tropical mean hydrological cycle (Fig. 2c). It accounts for almost the entire tropical mean moistening. It also increases the tropical mean precipitation at a higher rate than the fully coupled simulation due to the absence of atmospheric radiative warming associated with the direct CO_2 forcing. The tropical mean convection weakens at 3.5% K^{-1} under the mean SST warming, which accounts for about two-thirds of the total weakening. The effect of mean SST warming on the weakening of the mean circulation is very similar in the AMIP_mean and aqua_mean simulations, suggesting an insignificant impact of land–sea warming contrast on the tropical mean circulation weakening.

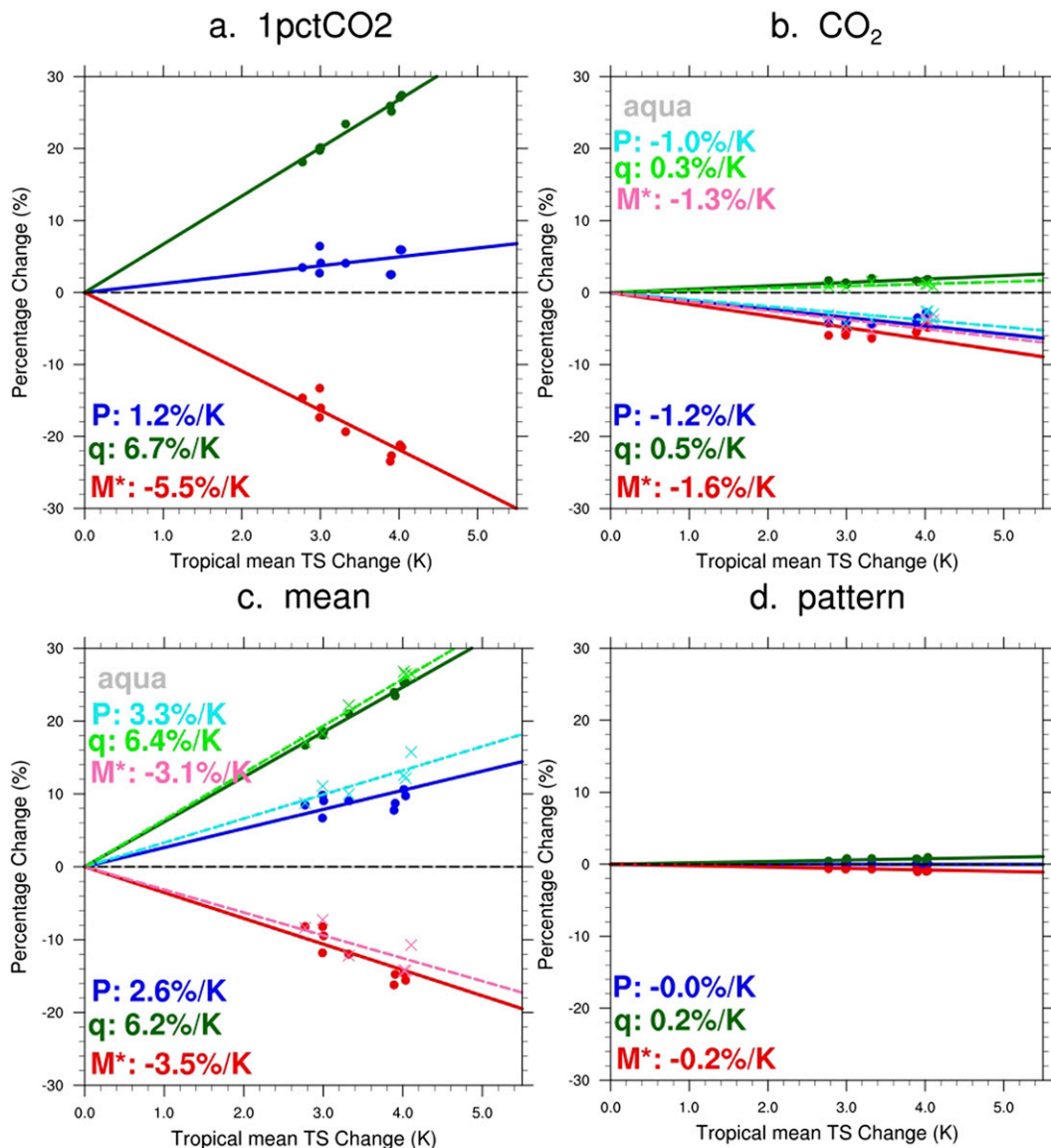From a dynamic viewpoint, the relative roles of direct CO_2 forcing, mean SST warming, and pattern of SST

FIG. 2. Tropical mean changes in precipitation (blue), moisture (green), and convective mass flux (red) from every model in the 1pctCO2 and AMIP simulations (dots) and the aquaplanet simulations (crosses) plotted against each model's tropical mean surface temperature changes in the 1pctCO2 simulation. The tropics are defined as the region between 30°S and 30°N. The lines indicate the ensemble mean changes, with solid lines representing the 1pctCO2 and the AMIP simulations and dashed lines representing the aquaplanet simulations. The text shows the ensemble mean changes after they are normalized by each model's tropical mean surface temperature changes in the 1pctCO2 simulation. Dark colors represent the 1pctCO2 and AMIP simulations and light colors represent the aquaplanet simulations.

warming on the weakening of the tropical mean circulation can be explained through changes in the tropospheric static stability (Knutson and Manabe 1995; Ma et al. 2012). In climate change simulations, the warming reaches a maximum in the upper troposphere. This tropical-wide increase in tropospheric static stability is commonly expected from the moist adiabatic adjustment (Knutson and Manabe 1995), although it is more

recently argued to be a vertical shift of the climatological temperature profile (O'Gorman and Singh 2013). Knutson and Manabe (1995) showed that the increased static stability allows for the weakening of convection while maintaining the balance between radiative cooling and convective heating. Ma et al. (2012) showed that the mean advection of the stratification change (MASC) acts as a weakening force on the overturning circulation
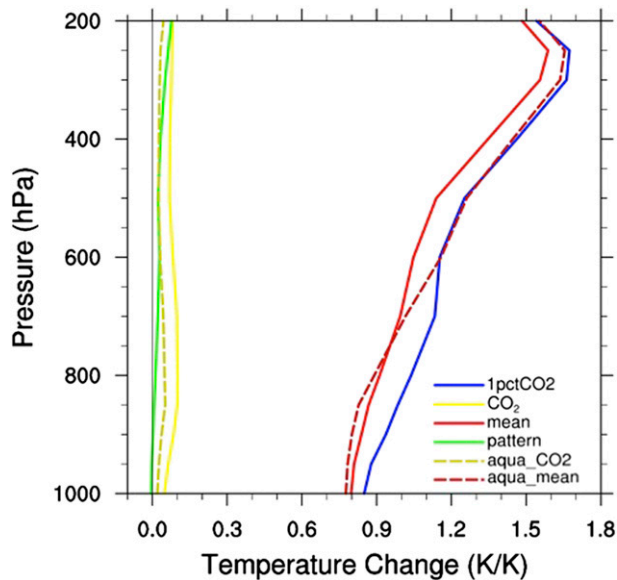
FIG. 3. Ensemble mean vertical profile of the horizontal mean temperature change from the 1pctCO2, AMIP, and aquaplanet simulations. The orange line is the sum of AMIP_CO2 and AMIP_mean. The tropics are defined as the region between 30°S and 30°N. Changes are normalized by each model's tropical mean surface temperature changes in the 1pctCO2 simulation before they are averaged across models to yield an ensemble mean.

and explains most of the total weakening of the Walker circulation and the Hadley cell, although the latter was partly counteracted by other factors. Based on these theories, we can evaluate the weakening effect of the forcing agents through the way they change the tropospheric static stability.

Figure 3 shows the change in tropospheric temperature in the 1pctCO2 simulation, the AMIP simulations and the aquaplanet simulations. Most of the tropospheric warming and static stability increase results from the mean SST warming, which increases the latent heat release in the free troposphere. The direct CO_2 forcing causes weak atmospheric warming and a small increase in static stability in the lower troposphere. The sum of AMIP_CO2 and AMIP_mean reproduces well the total warming in 1pctCO2. The warming effect of the pattern of SST change is even weaker, and is mostly in the high troposphere due to the anomalous convection associated with the enhanced equatorial warming (Xie et al. 2010). Overall, the individual impact of the forcing agents derived from changes in stratification is consistent with that from the thermodynamic theory by Held and Soden (2006).

b. Spatial pattern of tropical circulation change

Figure 4 shows the spatial pattern of changes in convective mass flux from the 1pctCO2 and AMIP

simulations. In the 1pctCO2 simulation (Fig. 4a), convection weakens almost everywhere in the tropics with the largest weakening in regions of climatological ascent, consistent with the MASC mechanism. On the other hand, convection strengthens over the equatorial Pacific, the northwest Indian Ocean, and the Indian peninsula. The increased convection over the equatorial Pacific and the northwest Indian Ocean is also found in the AMIP_pattern simulation and is therefore associated with the enhanced SST warming (Xie et al. 2010). The increased convection over the Indian peninsula is reproduced in the AMIP_CO2 simulation, in which land–sea warming contrast plays a role. Therefore, it is likely caused by the enhanced land warming, which favors the development of monsoonal rainfall.

The spatial change in convective mass flux in the 1pctCO2 simulation is well reproduced by the sum of AMIP_CO2, AMIP_mean, and AMIP_pattern, with a spatial correlation of 0.82 (Fig. 4b). Noticeable discrepancies exist over the southeast Pacific, the south equatorial Atlantic, and the northwest Indian monsoon region. Because of the different climatological SST in the 1pctCO2 and AMIP simulations, the discrepancies in convection change are likely caused by differences in the climatological convective mass flux, as the pattern of weakening closely follows the pattern of large climatological convection in both the 1pctCO2 and the sum of AMIP simulations (Ma et al. 2012; Chadwick et al. 2013a). These discrepancies may also be due to the differences in the pattern of SST change in AMIP_pattern and each coupled model.

In the AMIP_CO2 simulation (Fig. 4c), convection weakens over most of the tropical oceans. The weakening of convection is also produced in the aqua_CO2 simulation but with overall smaller magnitude (Fig. 5a). This indicates that the weakening in the AMIP_CO2 simulation is largely driven by the stabilization effect of increasing CO_2 but land–sea warming contrast may also play also an important role, which is consistent with the results from the solar experiment in Chadwick et al. (2014). In both the AMIP_CO2 and the aqua_CO2 simulations, the strongest weakening happens in regions of large climatological convection, suggesting that the MASC mechanism might also apply to circulation weakening in the CO_2 only simulations. The weakening effect of the direct CO_2 forcing certainly plays a role over land (Cao et al. 2012; Bony et al. 2013), but it is overpowered by the strengthening effect of the land surface warming.

The mean SST warming weakens convection almost everywhere in the tropics (Fig. 4d), with an overall larger magnitude than that from the direct CO_2 forcing. The strongest weakening is mainly found over the center

Changes in M* (kg/m²/s/K)

a. 1pctCO2

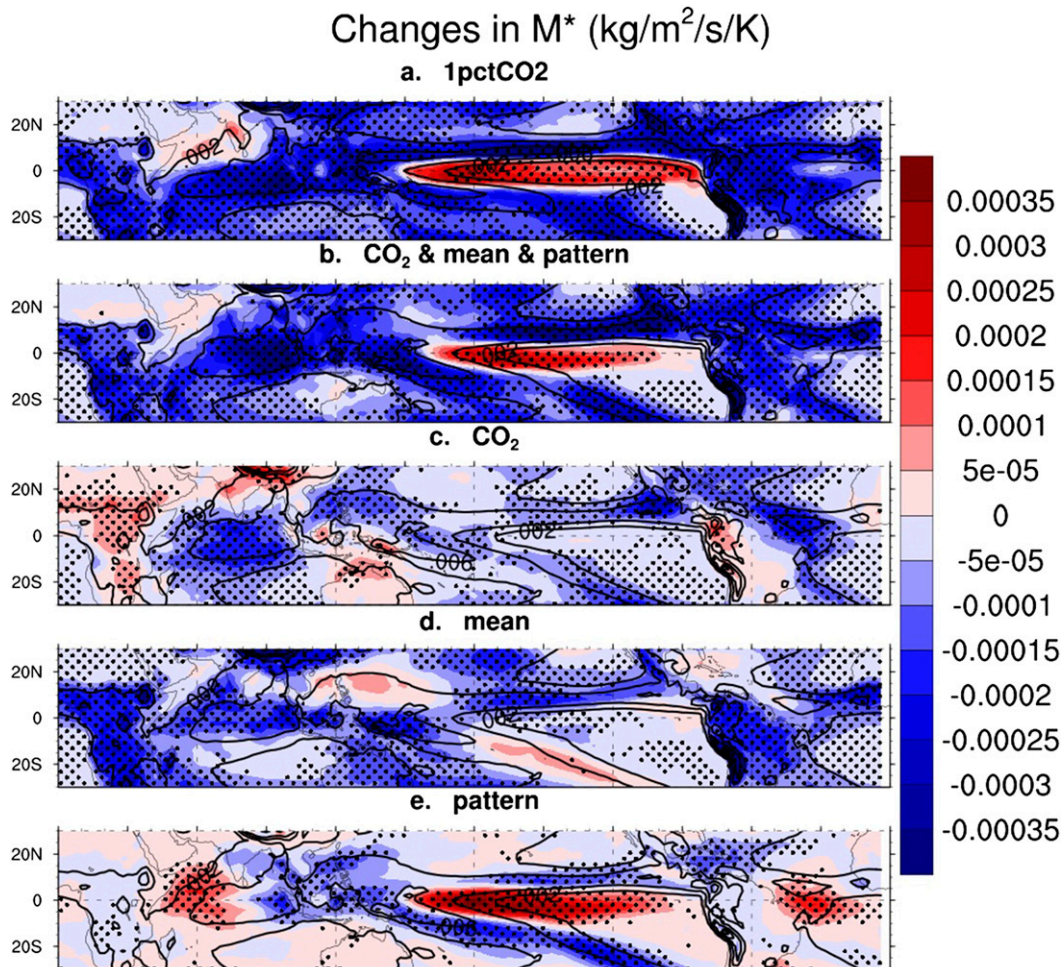### b. CO₂ & mean & pattern

c. CO₂

d. mean

e. pattern

FIG. 4. Ensemble mean changes in M^* (shading) superimposed on the climatological M^* (contour) from the (a) 1pctCO2 and (b)–(e) AMIP simulations. Changes are normalized by each model's tropical mean surface temperature changes in the 1pctCO2 simulation before they are averaged across models to yield an ensemble mean. Contour interval is $2 \times 10^{-3}\,\mathrm{kg^{-1}\,m^{-2}\,s^{-1}}$. Areas where at least 8 (out of 9) models agree on the sign of change are stippled.

of climatologically convective zones, consistent with previous studies (Ma et al. 2012; He et al. 2014). Strong weakening also happens at certain edges of convective zones, including the northwest Indian Ocean, the northern Pacific Ocean, and the equatorial Atlantic. This may likely reflect the "upped ante" mechanism, in which convection is suppressed through the advection of dry air from the less-moistened subsidence regions into the convective regions (Neelin et al. 2003; Chou et al. 2009). Despite the overall weakening, the mean SST warming also strengthens convection over the northwest Pacific and the eastern boundary of the South Pacific ITCZ. This may be associated with the increase of moisture in the lower troposphere, which overpowers the increase of dry static stability to yield a reduced gross moist stability (Chou and Neelin 2004; Chou et al. 2009).

However, the strengthening of convection is less robust among the CMIP5 models compared to the weakening of convection.

The weakening effect of the mean SST warming also dominates the pattern of convective mass flux change in the aqua_mean simulation. The strongest weakening happens over regions of large climatological convection, consistent with the AMIP_mean simulation. It is interesting that convection is strengthened at the equator (where convection is the strongest) in the aqua_mean simulation, although this is not a robust projection. The anomalous equatorial convection in the aqua_mean simulation could be driven dynamically by a positive moisture–convection feedback (Chou and Neelin 2004; Chou et al. 2009) or the anomalous equatorward surface wind associated with the weakening of convection off

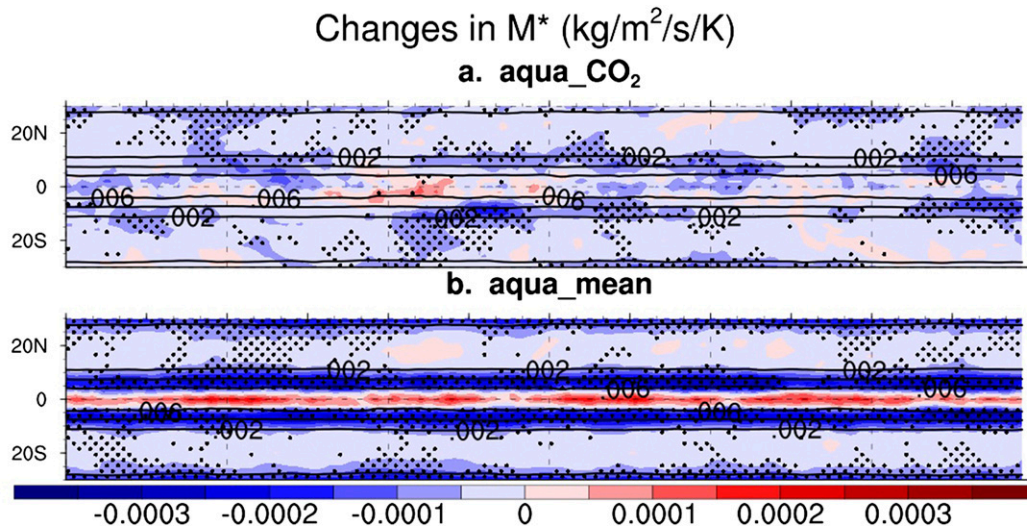## Changes in M* (kg/m²/s/K)

a. aqua_CO₂

b. aqua_mean

FIG. 5. Ensemble mean changes in M^* (shading) superimposed on the climatological M^* (contour) from the aquaplanet simulations. Changes are normalized by each model's tropical mean surface temperature changes in the 1pctCO2 simulation before they are averaged across models to yield an ensemble mean. Contour interval is $2 \times 10^{-3} \, kg^{-1} \, m^{-2} \, s^{-1}$. Areas where at least 5 (out of 6) models agree on the sign of change are stippled.

the equator; it could also be a result of internal variability due to the short length (5 yr) of the aquaplanet simulations.

The pattern of convection change in the AMIP_pattern simulation (Fig. 4e) generally follows the pattern of SST change (Fig. 1e), with increased convection over the warmest SST change and decreased convection over the less warm SST change. This "warmer-get-wetter" response reflects the changes in convective stability determined by the pattern of surface warming, as upper tropospheric warming is nearly uniform due to fast wave actions (Xie et al. 2010). Interestingly, the pattern of convection change caused by the pattern of SST warming generally opposes the climatological pattern of convection over the Pacific Ocean. Although this has little impact on the tropical mean convection, it weakens the pattern of convection by reducing its spatial variation.

This weakening effect of the pattern of SST warming can also be seen from the 500-hPa vertical velocity (Omega500; Fig. 6e): the anomalous convection weakens the descending motion at the equatorial and southeast Pacific, whereas the anomalous subsidence weakens the ascending motion at the Pacific ITCZ. It has been shown that the slowdown of equatorial surface wind causes an increase of ocean heat transport that warms the equatorial Pacific (DiNezio et al. 2009; Xie et al. 2010); here it is shown that the equatorial Pacific warming in turn enhances the weakening of the pattern of convection. Therefore, a positive feedback may very likely exist between the circulation weakening and the pattern of

SST change, although the mechanism behind this feedback needs further verification. On the other hand, the pattern of SST change has little impact on the convection over land, which is due to the insensitivity of Rossby wave generation associated with the pattern of SST change (He et al. 2014).

The direct CO_2 forcing, the mean SST warming, and the pattern of SST warming all act to weaken the tropical circulation spatially, as indicated by the negative spatial correlation between the changes in Omega500 and the climatological Omega500 in all three AMIP simulations (Fig. 7). Over land, the weakening is dominated by the mean SST warming (Fig. 7c). This is expected because most of the land warming happens in the AMIP_mean simulation (Fig. 1d) as a result of the ocean's remote influence on the water vapor and radiative feedback over land (Compo and Sardeshmukh 2009). On the other hand, land circulation strengthens in the AMIP_CO2 simulation due to the land–sea warming contrast.

Over ocean, all three forcing agents weaken the circulation, with the change in Omega500 generally opposing the climatological Omega500 (Figs. 7b–d). On the other hand, no single forcing agent is able to reproduce the total rate of weakening in Fig. 7a by itself. As shown in the maps of Omega500 (Fig. 6), much of the pattern of weakening over the tropical Pacific is reflected in the AMIP_pattern simulation, with anomalous ascent over the equatorial and southeast Pacific, and anomalous descent over the Pacific ITCZ. The weakening by the direct CO_2 forcing is most evident in
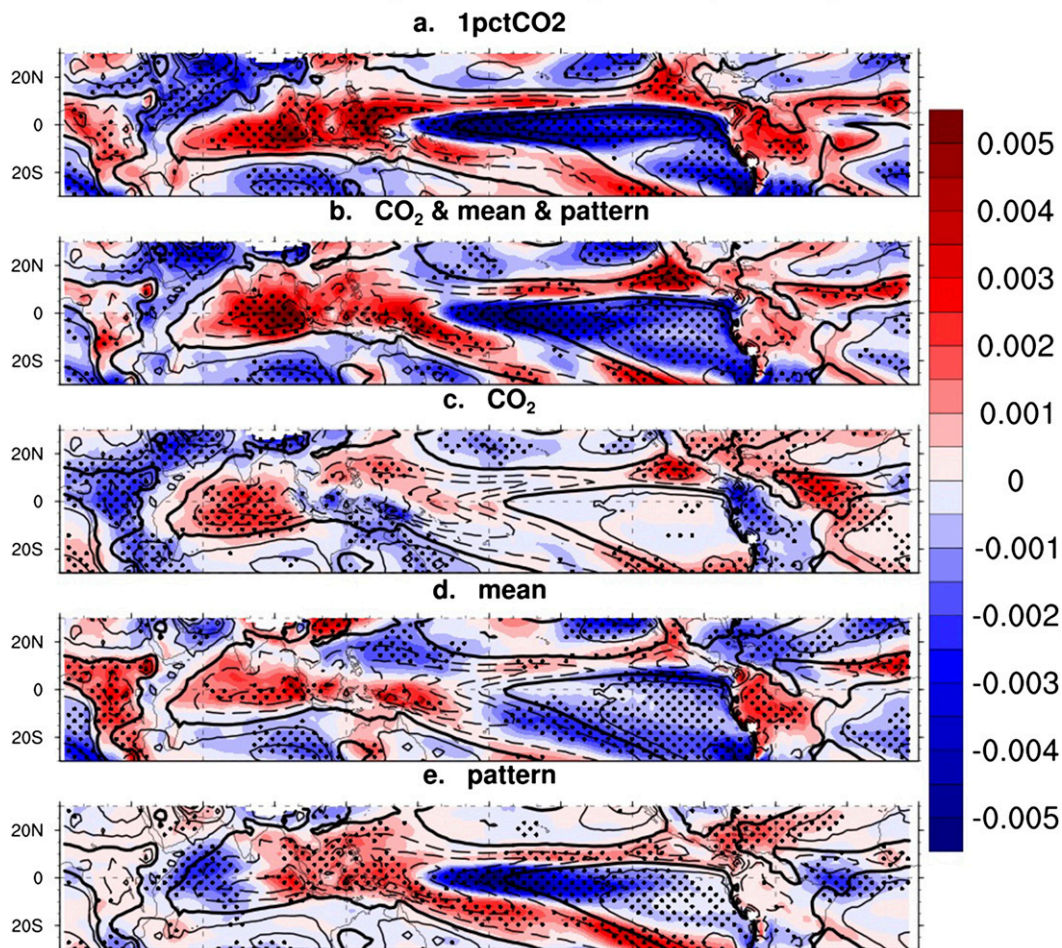
Changes in Omega500 (Pa/s/K)

a. 1pctCO2

b. CO$_2$ & mean & pattern

c. CO$_2$

d. mean

e. pattern

FIG. 6. As in Fig. 4, but for Omega500. Contour interval is 0.02 Pa s^{-1}. Zero contours are thickened.

convective zones over oceans, including the tropical Indian Ocean, the equatorial Atlantic, and the northeast Pacific. The mean SST warming weakens circulation over both ocean and land, with notable exceptions over the west Pacific ITCZ.

c. Weakening of the Walker circulation

It has been shown that the large-scale weakening of the tropical overturning circulation occurs primarily through the zonally asymmetric component of the circulation (Held and Soden 2006; Vecchi and Soden 2007), a key element of which is the Walker circulation. An anthropogenic weakening of the Walker circulation has been detected from both the upper-level velocity potential (e.g., Tanaka et al. 2004) and the large-scale zonal gradient of sea level pressure (SLP; e.g., Vecchi et al. 2006). Figure 8 shows a weakening and an eastward shift in the 200-hPa velocity potential from both the 1pctCO2 simulation and the sum of AMIP_CO2,

AMIP_mean, and AMIP_pattern, consistent with the findings of Vecchi and Soden (2007). The weakening is caused primarily by the mean SST warming (Fig. 8d), through the MASC mechanism and the feedback between convection and latent heat release (Ma et al. 2012). The eastward shift is mostly caused by the pattern of SST warming (Fig. 8e) through the enhanced SST warming at the central equatorial Pacific. It is interesting that the upper-level velocity potential does not weaken under an "El Niño–like" warming pattern (e.g., Liu et al. 2005; Xie et al. 2010; Ma and Xie 2013). This can be understood from the spatial structure of SLP response to the pattern of SST warming (Fig. 9e). The zonal SLP gradient is indeed reduced at the equator by the enhanced equatorial warming, but it drastically reverses its sign at about 10°S due to the minimum SST warming off the equator (Xie et al. 2010). Therefore, because of the narrow meridional structure of the warming pattern, the overall change in the zonal SLP gradient over the
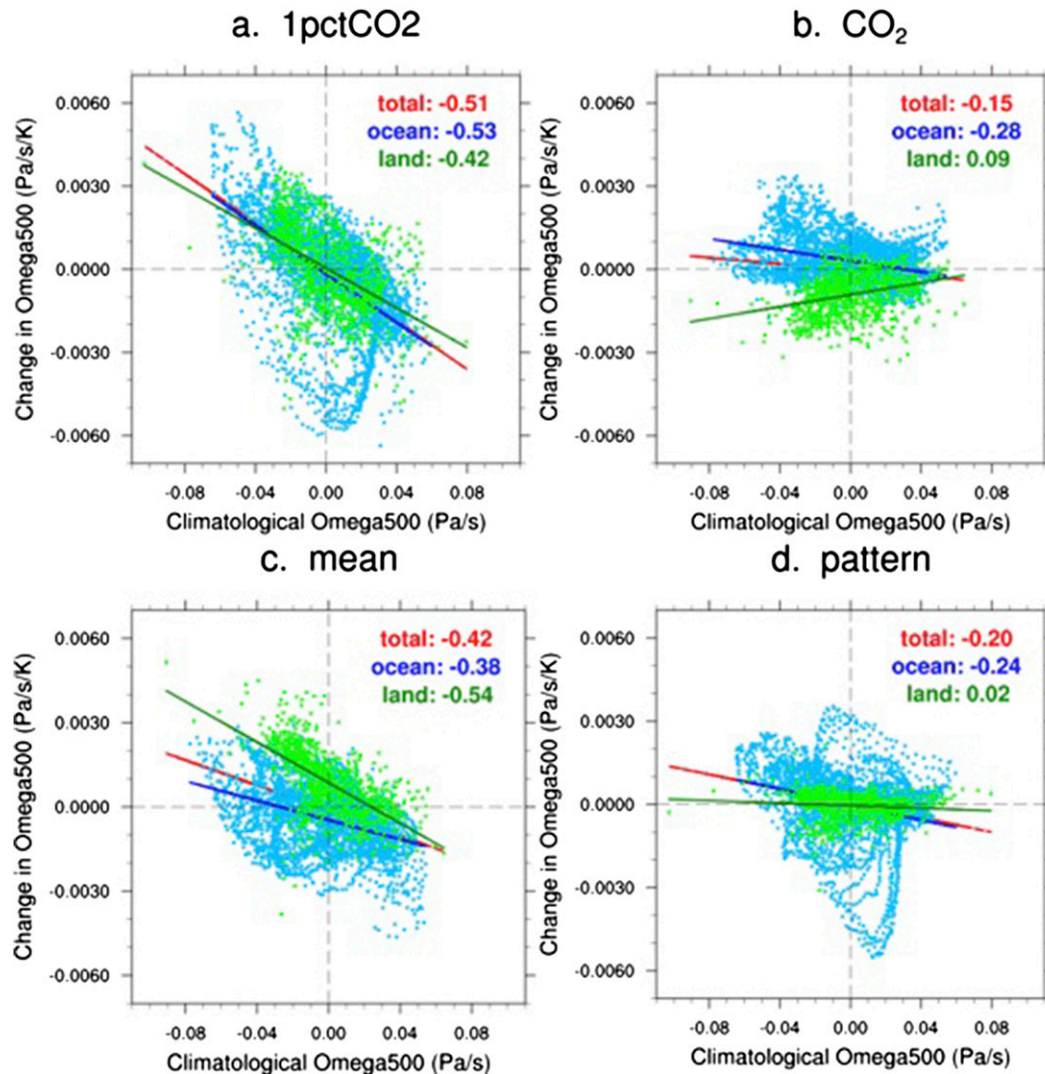
FIG. 7. Scatterplot of ensemble mean changes in Omega500 vs the climatological Omega500 from the 1pctCO2 and the AMIP simulations. Values are taken from a 2° × 2° grid. Ocean and land grid points are separated by color blue and green. The solid lines are the least squares fit to the data. Red lines represent all tropical grid points. The numbers in the top-right corner are the multimodel mean of the spatial correlation between changes in Omega500 and the climatological Omega500. The climatology in (d) is taken as the climatology in 1pctCO2 [as in (a)], as the pattern of SST change is calculated based on the 1pctCO2 simulation.

tropical Pacific is not enough to weakening the upper-level velocity potential, which represents the large-scale integral of circulation. This minor difference in the structure of SST responses to anthropogenic forcing and El Niño leads to very different responses in the Walker circulation, as well as other aspects of the atmospheric circulation (e.g., Lu et al. 2008; He et al. 2014).

In the AMIP_CO2 simulation, the 200-hPa velocity potential strengthens (Fig. 8c), consistent with the result from the GFDL model by Ma et al. (2012). Considering the fact that the direct CO_2 forcing weakens the circulation, the strengthening of the Walker circulation is

most likely caused by the land–sea warming contrast as an indirect effect of CO_2 (Fig. 1c). As shown in Fig. 9c, the warming of land relative to the ocean reduces SLP throughout the land while increasing SLP over most of the ocean (e.g., Bayr and Dommenget 2013). As a result, the zonal SLP gradient is increased between the eastern tropical Pacific and the western Pacific–Indonesian region, consistent with a strengthening of the Walker circulation. This shows the importance of land–sea warming contrast in regulating the Walker circulation. With our experimental design, we are unable to separate the effect of land–sea warming contrast and direct CO_2
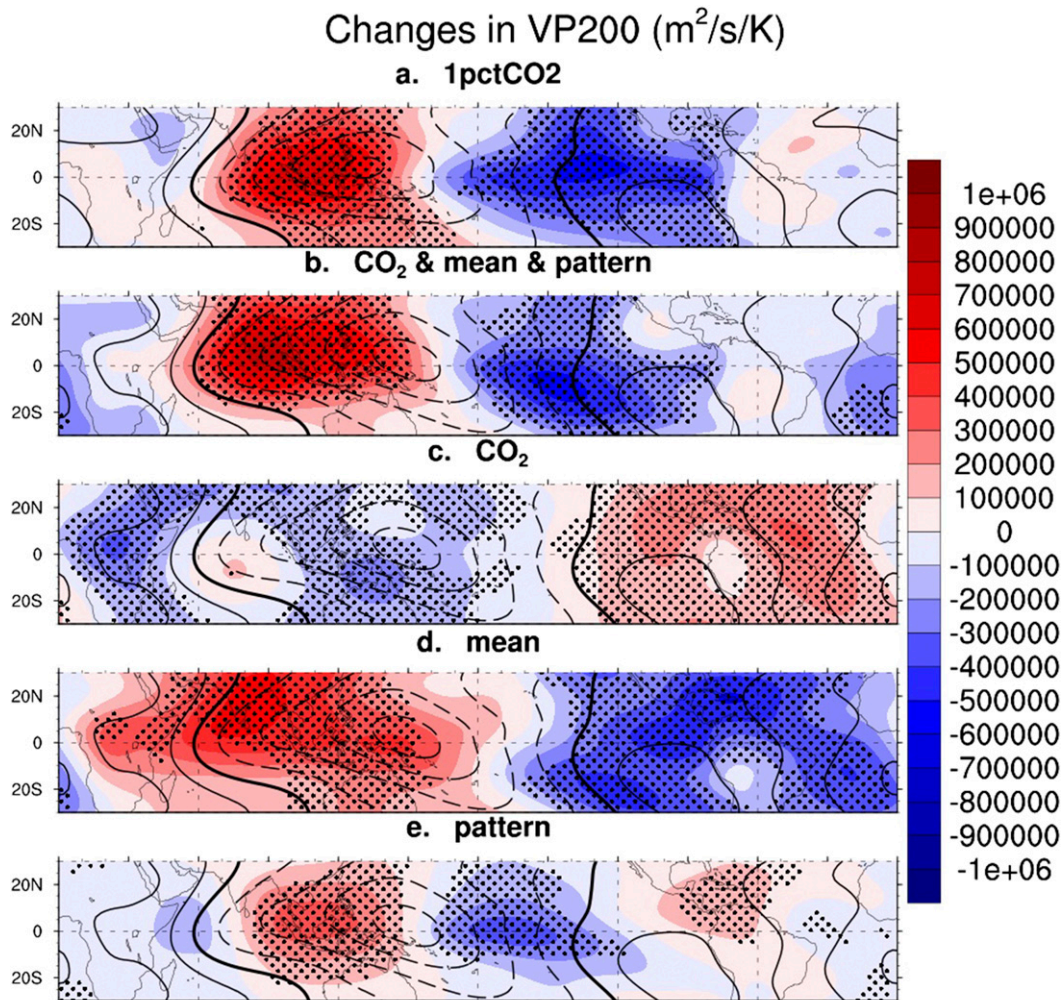
FIG. 8. As in Fig. 4, but for 200-hPa velocity potential. Contour interval is $3 \times 10^6 \, \mathrm{m \, s^{-1}}$.

forcing on the weakening of the Walker circulation. However, our results show that the weakening effect of direct CO_2 forcing could be overpowered by the strengthening effect of the fast land warming (as an indirect effect of CO_2 forcing) regarding changes in the Walker circulation.

d. Changes in the Hadley circulation

Despite the weakening in the zonally asymmetric component of tropical circulation, current CGCMs do not simulate a robust weakening in the meridional overturning circulation (e.g., Held and Soden 2006; Vecchi and Soden 2007; Ma and Xie 2013). Here we examine changes in the Hadley circulation by analyzing the zonal mean streamfunction (Fig. 10). In the 1pctCO2 simulation, the northern Hadley cell weakens, whereas the southern Hadley cell shows no consistent weakening or strengthening, which is in agreement with the results

from the CMIP3 ensemble (Ma and Xie 2013). However, in the sum of AMIP simulations both the northern and the southern cell weaken. The discrepancy between the 1pctCO2 and the sum of AMIP simulations could be due to either the differences in SST or nonlinearity of the responses to the forcing agents.

As shown in Fig. 10d, most of the weakening of the Hadley circulation is caused by the mean SST warming. In addition, the mean SST warming is responsible for the poleward shift of the boundary between the Hadley and Ferrel cells, which has been detected in model simulations (e.g., Lu et al. 2007; Frierson et al. 2007). The direct CO_2 weakens the Hadley cell in both hemispheres, although the weakening in the Southern Hemisphere is insubstantial. The pattern of SST change generally strengthens the Hadley circulation and shifts the center of the Hadley cell southward to the equator. This is mostly associated with the equatorial warming and the
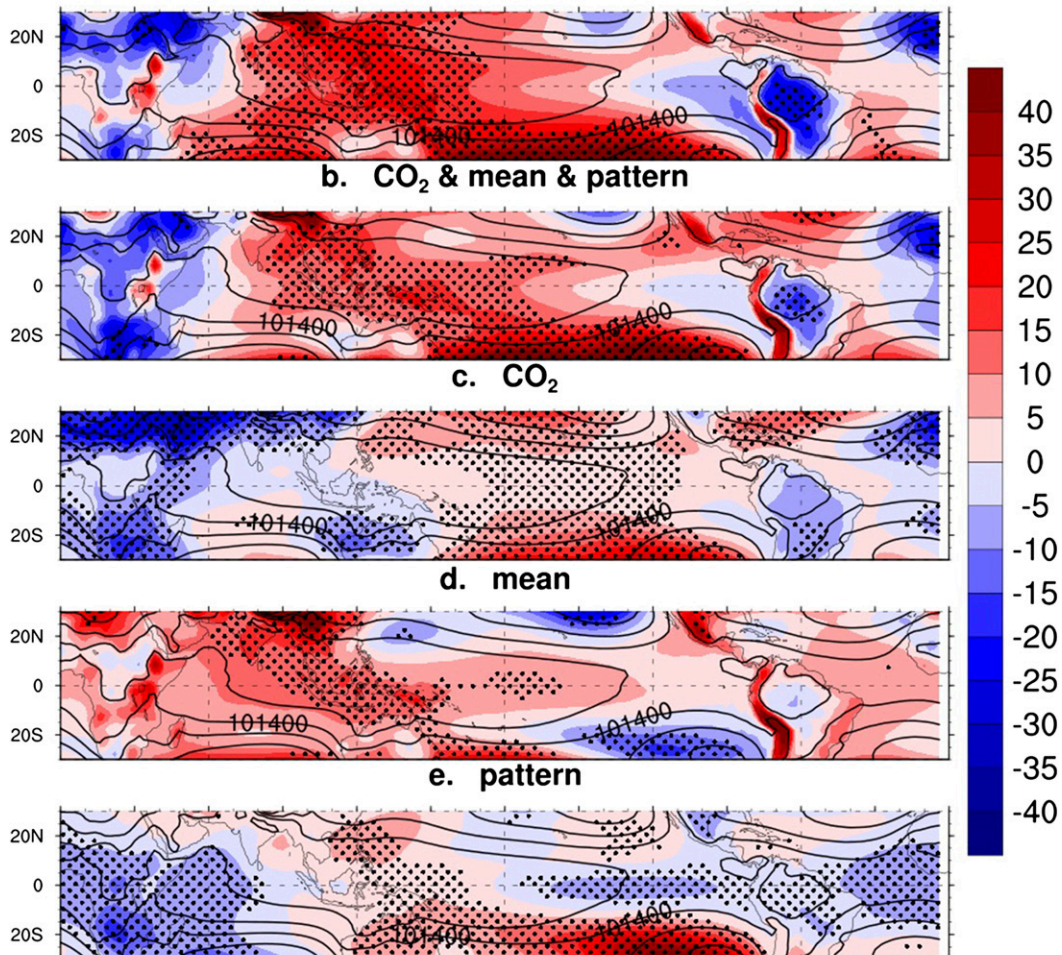
FIG. 9. As in Fig. 4, but for SLP. Contour interval is 300 Pa.

subtropical cooling in the Pacific (Ma and Xie 2013). Overall, the weakening effect from the mean SST warming overpowers the strengthening effect of the pattern of SST change, as indicated by the general weakening in the sum of AMIP simulations. Above 200 mb, the Hadley circulation strengthens, reflecting an increase in tropopause (e.g., Holzer and Boer 2001; Santer et al. 2003). This is mostly caused by the mean SST warming.

4. Conclusions

We have investigated the relative impacts of direct CO_2 forcing, mean SST warming, and the pattern of SST warming on the anthropogenic weakening of the tropical circulation using a nine-model ensemble of AMIP simulations, in which the three forcing agents were

specified individually. Overall, the sum of the AMIP simulations successfully reproduces the fully coupled simulation in terms of both the tropical mean weakening and the spatial pattern of weakening, giving justification to our approach.

For the weakening of the tropical mean circulation, the mean SST warming is the largest contributor through its dominance over changes in tropical mean precipitation and atmospheric moisture. The direct CO_2 forcing contributes moderately to the mean weakening through the radiative warming of the atmosphere. The pattern of SST warming has virtually no impact on the tropical mean hydrological cycle. The relative importance of the three forcing agents in the weakening of the tropical mean circulation can be dynamically explained through changes in the tropospheric stratification. The vertical profile of tropical mean temperature change
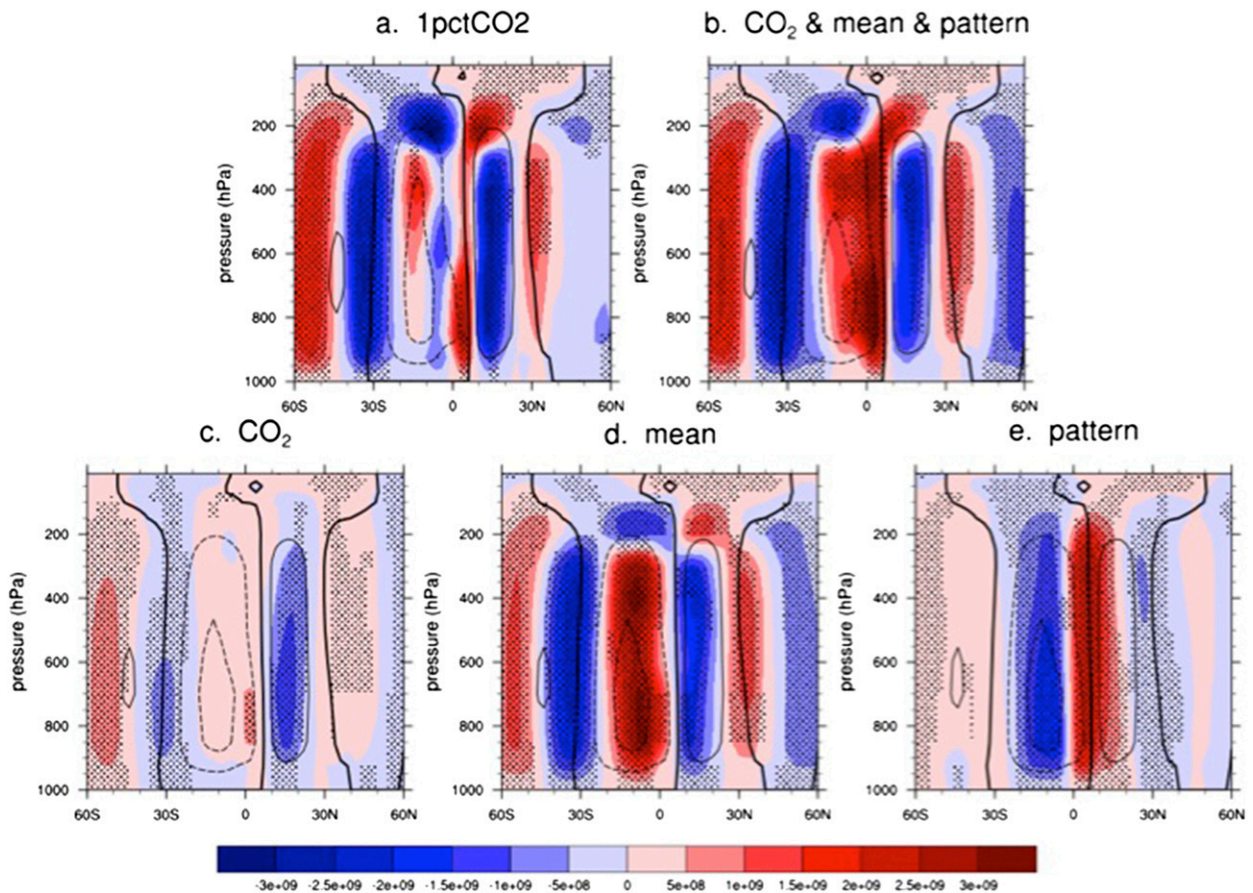
Zonal Mean psi (kg/s/K)

FIG. 10. Ensemble mean changes in zonal mean streamfunction (shading) superimposed on the climatology (contour) from the (a) 1pctCO2 and (b)–(e) AMIP simulations. Areas where at least 8 (out of 9) models agree on the sign of change are stippled. Contour interval is 4×10^{10} kg s^{-1}. Dashed contours indicate negative values. Zero contours are thickened.

showed that most of the increased tropospheric stratification is a result of the mean SST warming through its influence on the tropical mean moisture and latent heat release. In contrast, the direct CO_2 forcing only increases stratification moderately in the lower troposphere, whereas the pattern of SST warming has overall little impact.

In terms of the spatial pattern of circulation weakening, the direct CO_2 forcing, mean SST warming, and pattern of SST warming all contribute, especially over the ocean. The AMIP_CO2 simulation produces a weakening of convection over most of the tropical oceans with the largest weakening over convective zones. This weakening effect is a result of both the direct CO_2 forcing and the land–sea warming contrast, as the weakening is also simulated in the aquaplanet experiment but with a somewhat smaller magnitude. On the other hand, the increasing CO_2 strengthens convection over land by warming the land relative to

the ocean. The mean SST warming induces strong weakening of convection over both ocean and land. The weakening happens mostly at the center and the edge of convective zones. On the other hand, the mean SST warming also strengthens convection over certain convective regions in both the AMIP_mean and aqua_mean simulations, which is most likely driven by the positive moisture–convection feedback (Chou and Neelin 2004; Chou et al. 2009). The pattern of SST warming also contributes to the pattern of circulation weakening. This contribution is trivial over land but is very important over the tropical Pacific. It has been shown that the enhanced equatorial Pacific warming is closely linked to the weakening of surface wind (DiNezio et al. 2009; Xie et al. 2010). Our study indicates that the pattern of SST change could in turn influence circulation weakening. Such feedback may help better understand the anthropogenic changes in tropical circulation and SST.

We have also shown that the weakening of the Walker circulation is primarily caused by the mean SST warming. This is consistent with the study by Ma et al. (2012) using the GFDL model. Studies have shown that the pattern of SST change causes equatorial changes in precipitation and convection that resemble the characteristics of an El Niño event (e.g., Xie et al. 2010; He et al. 2014). However, changes in the upper-level velocity potential indicate that the pattern of SST warming has little impact on the weakening of the Walker circulation despite having an "El Niño–like" spatial structure. The narrow meridional width of the equatorial warming limits its impact on the large-scale zonal SLP gradient. The use of the AMIP_CO2 simulation maybe inadequate to evaluate the direct CO_2 impact on the Walker circulation, but our previous conclusion that the direct CO_2 forcing weakens circulation may shed some light on this issue. Nevertheless, it was shown that the increasing CO_2 could strengthen the Walker circulation indirectly by warming the land faster than the ocean, which could outweigh the weakening effect of the direct CO_2 forcing.

It has been shown that the pattern of SST change is the largest source of intermodel uncertainty in changes in the Hadley circulation (Ma and Xie 2013). But in terms of the ensemble mean response, we have shown that weakening effect of the mean SST warming generally overpowers the strengthening effect of the pattern of SST change. This results in a weakening of the Hadley cell in the sum of AMIP simulations. However, the coupled models do not simulate the weakening of the southern cell, which indicates that the response of the Hadley circulation could be nonlinear. In addition, the mean SST warming is also the main cause of the Hadley cell expansion and the lift of the tropopause.

REFERENCES

Allen, M. R., and W. J. Ingram, 2002: Constraints on future changes in climate and the hydrologic cycle. *Nature*, **419**, 224–232, doi:10.1038/nature01092.

Andrews, T., P. M. Forster, and J. M. Gregory, 2009: A surface energy perspective on climate change. *J. Climate*, **22**, 2557–2570, doi:10.1175/2008JCLI2759.1.

Bayr, T., and D. Dommenget, 2013: The tropospheric land–sea warming contrast as the driver of tropical sea level pressure changes. *J. Climate*, **26**, 1387–1402, doi:10.1175/JCLI-D-11-00731.1.

Boer, G., 1993: Climate change and the regulation of the surface moisture and energy budgets. *Climate Dyn.*, **8**, 225–239, doi:10.1007/BF00198617.

Bony, S., G. Bellon, D. Klocke, S. Sherwood, S. Fermepin, and S. Denvil, 2013: Robust direct effect of carbon dioxide on tropical circulation and regional precipitation. *Nature Geosci.*, **6**, 447–451, doi:10.1038/ngeo1799.

Bracco, A., F. Kucharski, R. Kallummal, and F. Molteni, 2004: Internal variability, external forcing and climate trends in multi-decadal AGCM ensembles. *Climate Dyn.*, **23**, 659–678, doi:10.1007/s00382-004-0465-2.

Cao, L., G. Bala, and K. Caldeira, 2012: Climate response to changes in atmospheric carbon dioxide and solar irradiance on the time scale of days to weeks. *Environ. Res. Lett.*, **7**, 034015, doi:10.1088/1748-9326/7/3/034015.

Chadwick, R., I. Boutle, and G. Martin, 2013a: Spatial patterns of precipitation change in CMIP5: Why the rich do not get richer in the tropics. *J. Climate*, **26**, 3803–3822, doi:10.1175/JCLI-D-12-00543.1.

——, P. Wu, P. Good, and T. Andrews, 2013b: Asymmetries in tropical rainfall and circulation patterns in idealised CO_2 removal experiments. *Climate Dyn.*, **40**, 295–316, doi:10.1007/s00382-012-1287-2.

——, P. Good, T. Andrews, and G. Martin, 2014: Surface warming patterns drive tropical rainfall pattern responses to CO_2 forcing on all timescales. *Geophys. Res. Lett.*, **41**, 610–615, doi:10.1002/2013GL058504.

Chou, C., and J. D. Neelin, 2004: Mechanisms of global warming impacts on regional tropical precipitation. *J. Climate*, **17**, 2688–2701, doi:10.1175/1520-0442(2004)017<2688:MOGWIO>2.0.CO;2.

——, ——, C. Chen, and J. Tu, 2009: Evaluating the "rich-get-richer" mechanism in tropical precipitation change under global warming. *J. Climate*, **22**, 1982–2005, doi:10.1175/2008JCLI2471.1.

Collins, M., and Coauthors, 2010: The impact of global warming on the tropical Pacific Ocean and El Niño. *Nat. Geosci.*, **3**, 391–397, doi:10.1038/ngeo868.

Compo, G., and P. D. Sardeshmukh, 2009: Oceanic influences on recent continental warming. *Climate Dyn.*, **32**, 333–342, doi:10.1007/s00382-008-0448-9.

Deser, C., and A. S. Phillips, 2009: Atmospheric circulation trends, 1950–2000: The relative roles of sea surface temperature forcing and direct atmospheric radiative forcing. *J. Climate*, **22**, 396–413, doi:10.1175/2008JCLI2453.1.

——, ——, V. Bourdette, and H. Teng, 2012: Uncertainty in climate change projections: The role of internal variability. *Climate Dyn.*, **38**, 527–546, doi:10.1007/s00382-010-0977-x.

DiNezio, P., A. C. Clement, G. Vecchi, B. J. Soden, B. P. Kirtman, and S.-K. Lee, 2009: Climate response of the equatorial Pacific to global warming. *J. Climate*, **22**, 4873–4892, doi:10.1175/2009JCLI2982.1.

Frierson, D. M. W., J. Lu, and G. Chen, 2007: Width of the Hadley cell in simple and comprehensive general circulation models. *Geophys. Res. Lett.*, **34**, L18804, doi:10.1029/2007GL031115.

He, J., and B. J. Soden, 2015: Does the lack of coupling in SST-forced atmosphere-only models limit their usefulness for climate change studies? *J. Climate*, doi:10.1175/JCLI-D-14-00597.1, in press.

——, ——, and B. Kirtman, 2014: The robustness of the atmospheric circulation and precipitation response to future

anthropogenic surface warming. *Geophys. Res. Lett.*, **41**, 2614–2622, doi:10.1002/2014GL059435.

Held, I. M., and B. J. Soden, 2006: Robust responses of the hydrological cycle to global warming. *J. Climate*, **19**, 5686–5699, doi:10.1175/JCLI3990.1.

Holzer, M., and G. J. Boer, 2001: Simulated changes in atmospheric transport climate. *J. Climate*, **14**, 4398–4420, doi:10.1175/1520-0442(2001)014<4398:SCIATC>2.0.CO;2.

Joshi, M. M., J. M. Gregory, M. J. Webb, D. M. H. Sexton, and T. C. Johns, 2008: Mechanisms for the land/sea warming contrast exhibited by simulations of climate change. *Climate Dyn.*, **30**, 455–465, doi:10.1007/s00382-007-0306-1.

Knutson, T. R., and S. Manabe, 1995: Time-mean response over the tropical Pacific to increased CO_2 in a coupled ocean–atmosphere model. *J. Climate*, **8**, 2181–2199, doi:10.1175/1520-0442(1995)008<2181:TMROTT>2.0.CO;2.

Kociuba, G., and S. B. Power, 2015: Inability of CMIP5 models to simulate recent strengthening of the Walker circulation: Implications for projections. *J. Climate*, **28**, 20–35, doi:10.1175/JCLI-D-13-00752.1.

Liu, Z., S. Vavrus, F. He, N. Wen, and Y. Zhong, 2005: Rethinking tropical ocean response to global warming: The enhanced equatorial warming. *J. Climate*, **18**, 4684–4700, doi:10.1175/JCLI3579.1.

Lu, J., G. A. Vecchi, and T. J. Reichler, 2007: Expansion of the Hadley cell under global warming. *Geophys. Res. Lett.*, **34**, L06805, doi:10.1029/2006GL028443.

——, G. Chen, and D. Frierson, 2008: Response of the zonal mean atmospheric circulation to El Niño versus global warming. *J. Climate*, **21**, 5835–5851, doi:10.1175/2008JCLI2200.1.

Ma, J., and S. Xie, 2013: Regional patterns of sea surface temperature change: A source of uncertainty in future projections of precipitation and atmospheric circulation. *J. Climate*, **26**, 2482–2501, doi:10.1175/JCLI-D-12-00283.1.

——, ——, and Y. Kosaka, 2012: Mechanisms for tropical tropospheric circulation change in response to global warming. *J. Climate*, **25**, 2979–2994, doi:10.1175/JCLI-D-11-00048.1.

Meng, Q., M. Latif, W. Park, N. S. Keenlyside, V. A. Semenov, and T. Martin, 2012: Twentieth century Walker circulation change: Data analysis and model experiments. *Climate Dyn.*, **38**, 1757–1773, doi:10.1007/s00382-011-1047-8.

Neelin, J. D., C. Chou, and H. Su, 2003: Tropical drought regions in global warming and El Nino teleconnections. *Geophys. Res. Lett.*, **30**, 2275, doi:10.1029/2003GL018625.

O'Gorman, P. A., and M. S. Singh, 2013: Vertical structure of warming consistent with an upward shift in the middle and upper troposphere. *Geophys. Res. Lett.*, **40**, 1838–1842, doi:10.1002/grl.50328.

Power, S. B., and I. N. Smith, 2007: Weakening of the Walker Circulation and apparent dominance of El Niño both reach record levels, but has ENSO really changed? *Geophys. Res. Lett.*, **34**, L18702, doi:10.1029/2007GL030854.

——, and G. Kociuba, 2011: What caused the observed twentieth-century weakening of the Walker circulation? *J. Climate*, **24**, 6501–6514, doi:10.1175/2011JCLI4101.1.

Santer, B. D., and Coauthors, 2003: Contributions of anthropogenic and natural forcing to recent tropopause height changes. *Science*, **301**, 479–483, doi:10.1126/science.1084123.

Soden, B. J., 2000: The sensitivity of the tropical hydrological cycle to ENSO. *J. Climate*, **13**, 538–549, doi:10.1175/1520-0442(2000)013<0538:TSOTTH>2.0.CO;2.

Tanaka, H. L., N. Ishizaki, and A. Kitoh, 2004: Trend and interannual variability of Walker, monsoon and Hadley circulations defined by velocity potential in the upper troposphere. *Tellus*, **56A**, 250–269, doi:10.1111/j.1600-0870.2004.00049.x.

Taylor, K. E., R. J. Stouffer, and G. A. Meehl, 2012: An overview of CMIP5 and the experiment design. *Bull. Amer. Meteor. Soc.*, **93**, 485–498, doi:10.1175/BAMS-D-11-00094.1.

Thorpe, L., and T. Andrews, 2014: The physical drivers of historical and 21st century global precipitation changes. *Environ. Res. Lett.*, **9**, 064024, doi:10.1088/1748-9326/9/6/064024.

Tokinaga, H., S.-P. Xie, C. Deser, Y. Kosaka, and Y. M. Okumura, 2012: Slowdown of the Walker circulation driven by tropical Indo-Pacific warming. *Nature*, **491**, 439–443, doi:10.1038/nature11576.

Vecchi, G. A., and B. J. Soden, 2007: Global warming and the weakening of the tropical circulation. *J. Climate*, **20**, 4316–4340, doi:10.1175/JCLI4258.1.

——, ——, A. T. Wittenberg, I. M. Held, A. Leetmaa, and M. J. Harrison, 2006: Weakening of tropical Pacific atmospheric circulation due to anthropogenic forcing. *Nature*, **441**, 73–76, doi:10.1038/nature04744.

Xie, S.-P., C. Deser, G. A. Vecchi, J. Ma, H. Teng, and A. T. Wittenberg, 2010: Global warming pattern formation: Sea surface temperature and rainfall. *J. Climate*, **23**, 966–986, doi:10.1175/2009JCLI3329.1.